Theoretical Study of Pyridine and 4,4′-Bipyridine Adsorption on the Lewis Acid Sites of Alumina Surfaces Based on Ab Initio and Density Functional Cluster Calculations

Emile Kassab*,† and Martine Castellà-Ventura‡

Laboratoire de Chimie Théorique, CNRS-UMR 7616, Université Pierre et Marie Curie, Tour 22-23, Case 137, 4 place Jussieu, 75252 Paris Cedex 05, France, and Laboratoire de Dynamique, Interactions et Réactivité, CNRS−UMR 7075, 2 Rue Henry Dunant, 94320 Thiais, France

Received: July 31, 2004

The interactions of pyridine and 4,4′-bipyridine with the Lewis acid sites of alumina surfaces are investigated using ab initio and density functional calculations. Four cluster models of different sizes and shapes are chosen to represent the Lewis acid sites: three hydrogenated clusters $Al(OH)_3$, $Al_4O_9H_6$, and $Al_{10}O_{21}H_{12}$ and one non-hydrogenated cluster Al_4O_6. The Hartree−Fock (HF) and B3LYP approaches with two basis sets 6-31G* and 6-31+G* are used to calculate the geometries, the electronic structures, the vibrational frequencies, and the adsorption energies of the complexes formed upon interaction of pyridine or 4,4′-bipyridine ligands on the cluster surfaces. Electronic structures are determined by the electrostatic potential (ESP) analysis of charges. Adsorption energies are calculated with corrections made for zero-point energies (ZPE) and basis set superposition error (BSSE). The ESP analysis of atomic charges reveals that the charge-transfer effects are more important in Lewis complexes formed with Al_4O_6 cluster than in those formed with hydrogenated clusters $Al(OH)_3$, $Al_4O_9H_6$, and $Al_{10}O_{21}H_{12}$. The significantly larger charge transferred from pyridine or 4,4′-bipyridine ligand to Al_4O_6 cluster should increase the adsorption energy of these complexes. Consequently, at all levels of calculation, the adsorption energies of pyridine and 4,4′-bipyridine complexed to Al_4O_6 cluster (∼46 kcal/mol), which compare very well to experiment, are strongly larger than those obtained for both pyridine and 4,4′-bipyridine ligands complexed to $Al(OH)_3$ (32 kcal/mol), $Al_4O_9H_6$ (24 kcal/mol) and $Al_{10}O_{21}H_{12}$ (25 kcal/mol) clusters. The corrected adsorption energy is found to be insensitive to basis set and electron correlation effects. It essentially depends on the ionic character of the cluster model rather than on its size. For 4,4′-bipyridine complexes, similar results to those obtained for pyridine are found, and the geometry and the amount of charge of the unbound pyridyl ring are unchanged upon complexation. The calculated vibrational frequencies and frequency shifts are little sensitive to the size and shape of the cluster model. The two ring stretching modes 8a and 19b of pyridine and 4,4′-bipyridine observed in the 1400−1600 cm^{-1} region are the most affected modes upon adsorption, in good agreement with the available infrared and Raman data.

I. Introduction

Alumina (Al_2O_3) is an ionic metal oxide of considerable interest in catalysis. It may act both as a catalyst and as a support of active species.[1] It is also widely used in microelectronics as dielectrics.[2] The catalytic activity of aluminum oxide is explained, as in the general case of metal oxides, by its surface acid−base properties.

The different active sites of alumina result from adsorption and desorption of water, which is always present in the surrounding medium. Hydroxy-groups arise from dissociative adsorption of water molecules; they act either as Brönsted acid sites or as hydrogen-bond donor. Coordinately unsaturated cations (Al^{3+}) and anions (O^{2-} and OH^-) result from thermal dehydroxylation of alumina; they form the Lewis acid and base sites, respectively.[6−8] The characterization of the acid−base properties, i.e., the concentration, the nature (Brönsted or Lewis), and the strength of the active sites, has been extensively investigated by various experimental techniques, particularly by the Fourier transform infrared (FT-IR) spectroscopy of adsorbed specific probe molecules,[1,3−6] such as ammoniac, pyridine (PY), acetonitrile, nitrogen monoxide, carbon monoxide, and carbon dioxide molecules.[9−23] This method is based on the identification of the vibrational modifications (frequencies, intensities) undergone by the probe molecule upon adsorption on the surface. Pyridine has been largely used as a probe molecule of metal oxide surfaces,[3,5,6,10−23,82] since it allows differentiating the Lewis and Brönsted acid sites.[1,5−6,15] Its ring-stretching vibrational modes, mostly modes 8a and 19b, located between 1400 and 1700 cm^{-1}, are particularly affected upon complexation.[4,5,15,22,23] Pyridine coordinately bonded to surface Lewis acid sites gives rise to infrared (IR) bands at 1600−1635 cm^{-1} (mode 8a) and at 1440−1460 cm^{-1} (mode 19b), whereas pyridinium cations PyH^+ on surface protonic Brönsted acid sites leads to observed bands at 1535−1550 cm^{-1} and about 1640 cm^{-1}. Only Lewis acidity has been generally evidenced on alumina from spectroscopic studies of PY adsorption.[10,14,15,17,21] The concentration of Lewis acid sites is determined from the intensity of the 19b band.[11] The strength and the number of the different types of Lewis acid sites are deduced from the shift and the multiplicity of the 8a band.[12−14,82] The more the 8a frequency is upward shifted, the stronger the Lewis acid site.

PY, as the other probe molecules previously quoted, are monodentate systems, which only allow the characterization of

* To whom correspondence should be addressed. E-mail: ek@lct.jussieu.fr.
† Université Pierre et Marie Curie.
‡ CNRS−UMR 7075.

10.1021/jp040524b CCC: $30.25
Published on Web 06/25/2005

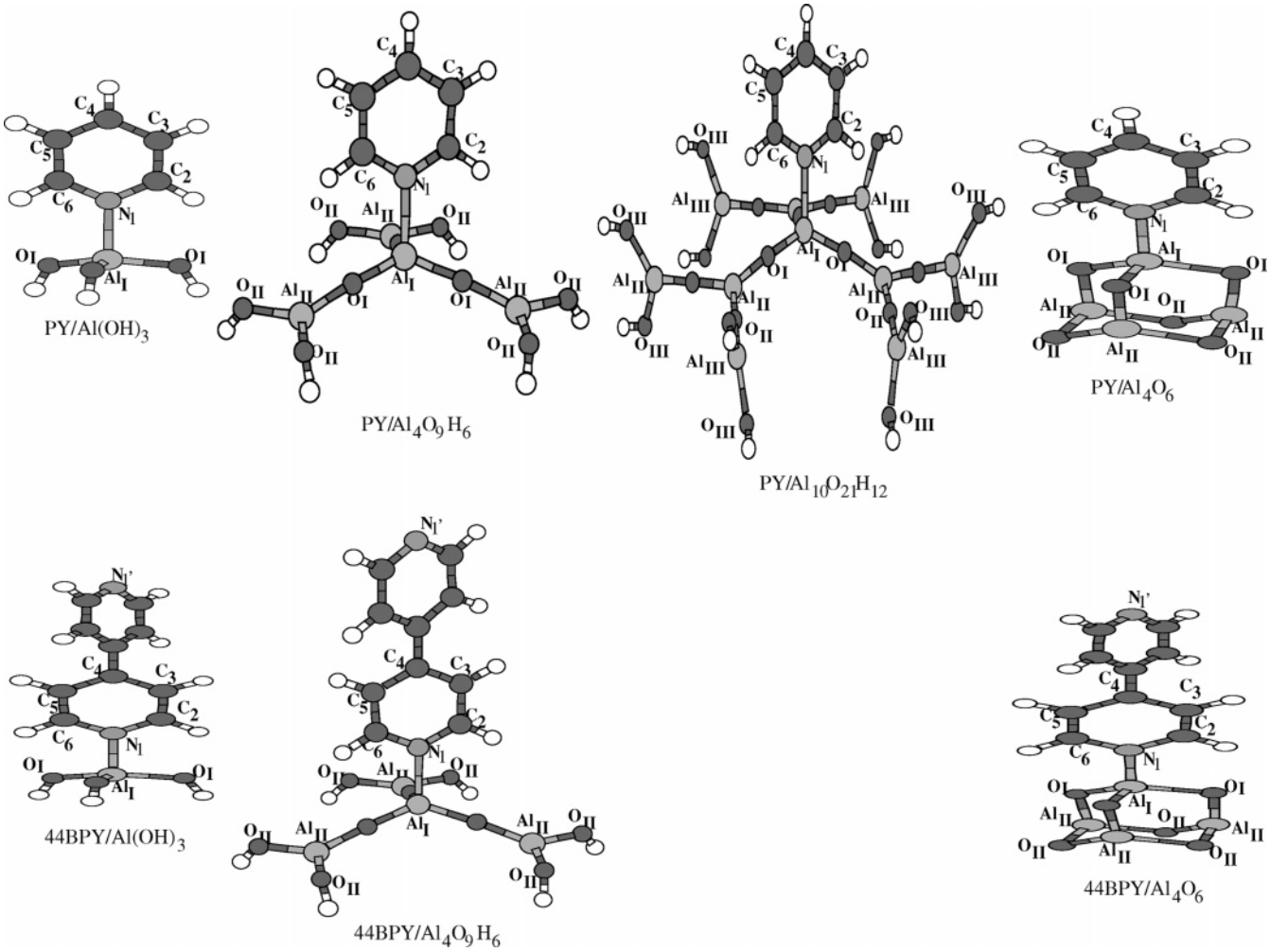

Figure 1. Pyridine and 4,4′-bipyridine ligands complexed to the Al Lewis acid site of alumina clusters.

a single surface acid site. In the past decade, Bagshaw and Cooney[24] extend the FT-IR spectral probe method to the adsorption of bidentate molecules, such as bipyridines (2,2′-bipyridine[25] and 4,4′-bipyridine (44BPY)[26]), which permit to simultaneously characterize more than one acid site and to determine the distance between the different active sites.

Many theoretical works based on quantum-mechanical methods, mostly in the ab initio or density functional theory (DFT) framework, have been devoted to the energetic, and in scarce cases, vibrational characterization of the probe molecule-alumina surface interaction.[8,9,27−42,83] All studies concern small adsorbed species, principally water,[8,27−33,40,42,83] but also ammonia,[34,42] hydrogen chloride,[35a] carbon monoxide,[36−40] acetonitrile,[9] and hydrogen sulfide,[40,41] except one bearing on a larger probe system, the PY molecule.[42,91] The alumina surface may be treated with two types of quantum chemistry methods. First, the periodic calculations using both Hartree−Fock (HF) and DFT methods[45] allow studying the full structure of the metal oxide surface. Second, the finite cluster method,[27−44] generally employed, permits to restrict the surface to a fragment, which properties approximately mimic those of the whole surface. As the cluster is formed from the breaking of bonds between the fragment and the remainder of the metal oxide, the charge distribution in the cluster may be disturbed. To remedy to this, the dangling bonds are saturated with hydrogen atoms.[46] To take into consideration the long-range Coulombic effects (Madelung potential) due to the rest of the metal oxide, the cluster may be embedded in a field of point charges.[30−33,38]

We present in this paper the first theoretical study of the adsorption interactions of aza-aromatic molecules (PY and 44BPY) with the Lewis acid sites of alumina surfaces by using ab initio and DFT calculations in the cluster model framework. Four neutral cluster models of different size and shape have been chosen to simulate the tricoordinate aluminum active site of the alumina surface (Figure 1). The small cluster $Al(OH)_3$, the medium size cluster $Al_4O_9H_6$, and the larger size cluster $Al_{10}O_{21}H_{12}$ have dangling bonds terminated with hydrogen saturators. The fourth cluster Al_4O_6, non-hydrogenated, is the same stoechiometric cluster yet employed by Wittbrodt et al.[30] to investigate molecular and 1−2 dissociative adsorption of water. For each interaction of PY or 44BPY with a cluster, we have calculated (i) the modifications of geometrical and electronic structures undergone by the adsorbed molecule and the cluster, (ii) the adsorption energies of the complexes, and (iii) the vibrational spectra of the adsorbed molecule, which have been analyzed (eigenvectors, frequencies, and potential energy distributions (PEDs)) and compared with the free molecule spectra.

II. Computational Details

The quantum chemical calculations were carried out at the HF level, and with the DFT method at the B3LYP level, using two basis sets 6-31G* and 6-31+G*. The geometries were optimized by using the standard techniques implemented in the Gaussian 98 package.[47] Except for the hydrogenated clusters and their complexes, no symmetry constraints were assumed at

TABLE 1: Local Symmetry Coordinates of PY and 44BPY, as Recommended by Pulay et al.[51a]

definition	description
In-Plane Coordinates[b]	
R_1,R_6,R'_1,R'_6	CN stretching
$R_2,R_3,R_4,R_5,R'_2,R'_3,R'_4,R'_5$	CC stretching
R	inter-ring stretching
$r_2,r_3,r_5,r_6,r'_2,r'_3,r'_5,r'_6$	CH stretching
r_4	CH stretching[c]
$\beta_i = b_i\text{-}c_i$, $\beta'_i = b'_i\text{-}c'_i$; i=2,3,5,6	CH in-plane bending
$\beta_4 = b_4\text{-}c_4$	CH in-plane bending[c]
$\beta_4 = b_4\text{-}c_4$, $\beta'_4 = b'_4\text{-}c'_4$	C-ring in-plane bending[d]
$S_1=a_1\text{-}a_2+a_3\text{-}a_4+a_5\text{-}a_6$, $S'_1=a'_1\text{-}a'_2+a'_3\text{-}a'_4+a'_5\text{-}a'_6$	ring in-plane deformation
$S_2=2a_1\text{-}a_2\text{-}a_3+2a_4\text{-}a_5\text{-}a_6$, $S'_2=2a'_1\text{-}a'_2\text{-}a'_3+2a'_4\text{-}a'_5\text{-}a'_6$	ring in-plane deformation
$S_3=a_2\text{-}a_3+a_5\text{-}a_6$, $S'_3=a'_2\text{-}a'_3+a'_5\text{-}a'_6$	ring in-plane deformation
Out-of-Plane Coordinates[b]	
$\gamma_2,\gamma_3,\gamma_5,\gamma_6,\gamma'_2,\gamma'_3,\gamma'_5,\gamma'_6$	CH out-of-plane bending
γ_4	CH out-of-plane bending[c]
γ_4,γ'_4	C-ring out-of-plane bending[d]
$S_4=t_{12}\text{-}t_{23}+t_{34}\text{-}t_{45}+t_{56}\text{-}t_{61}$, $S'_4=t'_{12}\text{-}t'_{23}+t'_{34}\text{-}t'_{45}+t'_{56}\text{-}t'_{61}$	ring out-of-plane deformation
$S_5=t_{12}-2t_{23}+t_{34}+t_{45}-2t_{56}+t_{61}$, $S'_5=t'_{12}-2t'_{23}+t'_{34}+t'_{45}-2t'_{56}+t'_{61}$	ring out-of-plane deformation
$S_6=t_{12}\text{-}t_{34}+t_{45}\text{-}t_{61}$, $S'_6=t'_{12}\text{-}t'_{34}+t'_{45}\text{-}t'_{61}$	ring out-of-plane deformation
ω	inter-ring torsion[d]

[a] The atom numbering and the notation of the internal coordinates are given in Figure 2. [b] The prime coordinates only concern 44BPY. [c] This coordinate only concerns PY. [d] These coordinates only concern 44BPY.

the beginning of each geometry optimization. However, in the case where the optimization ended with a nearly symmetric structure, the system symmetry was verified. Harmonic vibrational frequencies were calculated to confirm the nature of the stationary points and to provide the vibrational zero-point energy (ZPE). For the hydrogenated clusters $Al(OH)_3$, $Al_4O_9H_6$, and $Al_{10}O_{21}H_{12}$ and their complexes, to preclude the formation of intramolecular hydrogen bonds, only the AlOH torsional angles were assumed to be frozen during the optimization. The atomic net charges for all systems considered were deduced from electrostatic potential (ESP) calculations which utilize the Breneman−Wiberg approximation.[48] These atomic charges were used to calculate the charge transferred between two fragments interacting in the Lewis complexes.

Interaction energy, here called adsorption energy, was computed as the difference between the energy of the optimized adsorption complex, i.e., molecule-cluster, and the sum of energies of optimized isolated fragments molecule and cluster. Corrections to the adsorption energies for the basis set superposition error (BSSE) were estimated by the counterpoise method.[49] The frequencies computed for all species studied here were scaled by our scaling factors (see below) determined to give the best agreement between the experimental anharmonic and the calculated frequencies for PY and 44BPY free molecules and their complexes.

The force constants for the Cartesian displacements were obtained at each level of calculation by analytical differentiation algorithms included in the Gaussian 98 program.[47] The transformation of the Cartesian force fields to force fields in local symmetry coordinates for each vibrational mode was carried out by employing the REDONG program.[50] These nonredundant symmetry coordinates (Table 1) were defined as recommended by Pulay et al.[51] They were expressed as a function of the internal coordinates shown in Figure 2. The PEDs were calculated for each vibrational mode from the force constants expressed in local symmetry coordinates. To designate the normal modes of PY and 44BPY, we used the convention adopted by Varsanyi for monosubstituted benzenes,[84] adapted from the Wilson notation for benzene.[85]

For reasons of space, not all of the optimized geometrical and vibrational results are reported here. They will be furnished on request.

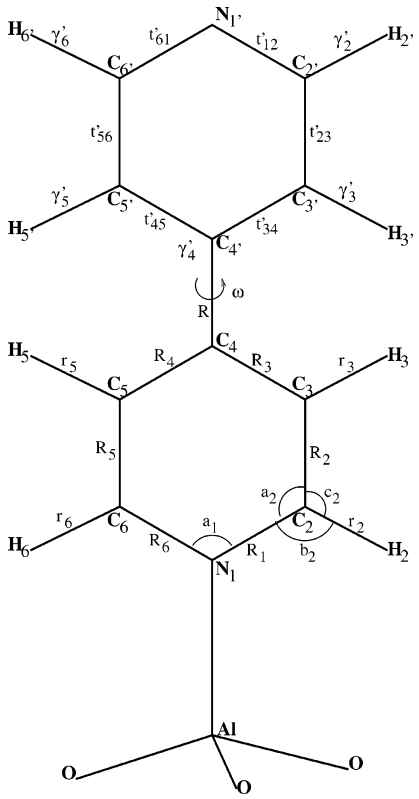

Figure 2. Atom numbering and internal coordinates of 4,4′-bipyridine adsorbed on an alumina cluster. For pyridine, the prime ring is replaced by hydrogen atom (H_4).

III. Results and Discussion

A. Structures. The main optimized geometrical parameters determined at the HF and B3LYP levels with 6-31G* and 6-31+G* basis sets of PY and 44BPY free and adsorbed molecules onto the four cluster models $Al(OH)_3$ and $Al_4O_9H_6$, $Al_{10}O_{21}H_{12}$ and Al_4O_6 are presented and compared with available experimental data in Tables 2 and 3, respectively. The different AlO distances of the four clusters, free or into the complexes with PY and 44BPY, optimized with the HF and B3LYP methods using 6-31G* and 6-31+G* basis sets are given in Table 4. Structures for molecular adsorption of PY

TABLE 2: Geometrical Parameters of PY and Its Lewis Complexes with Alumina Clusters Optimized at HF and B3LYP Levels with the 6-31G* and 6-31+G* (in Brackets) Basis Sets

	PY			$PY/Al(OH)_3$		$PY/Al_4O_9H_6$		$PY/Al_{10}O_{21}H_{12}$		PY/Al_4O_6	
bond lengths/Å	exp[a]	HF	B3LYP	HF	B3LYP	HF	B3LYP	HF	B3LYP	HF	B3LYP
N_1C_2	1.338	1.321	1.339	1.330	1.347	1.329	1.346	1.332	1.350	1.332	1.349
		(1.322)	(1.341)	(1.331)	(1.348)	(1.330)	(1.347)			(1.332)	(1.349)
C_2C_3	1.394	1.385	1.396	1.379	1.391	1.379	1.390	1.378	1.390	1.378	1.390
		(1.386)	(1.397)	(1.381)	(1.392)	(1.381)	(1.392)			(1.379)	(1.390)
C_3C_4	1.392	1.384	1.395	1.385	1.395	1.385	1.395	1.386	1.396	1.386	1.396
		(1.386)	(1.397)	(1.386)	(1.396)	(1.386)	(1.396)			(1.387)	(1.397)
Al_IN_1				2.003	2.005	2.043	2.028	2.065	2.047	1.968	1.970
				(2.000)	(1.998)	(2.048)	(2.036)	(2.073)	(2.061)	(1.964)	(1.967)

[a] Reference 58.

TABLE 3: Geometrical Parameters of 44BPY and Its Lewis Complexes with Alumina Clusters Optimized at HF and B3LYP Levels with the 6-31G* and 6-31+G* (in Brackets) Basis Sets

geometrical parameters	44BPY			$44BPY/Al(OH)_3$		$44BPY/Al_4O_9H_6$		$44BPY/Al_4O_6$	
	exp[b]	HF	B3LYP	HF	B3LYP	HF	B3LYP	HF	B3LYP
				Bond Lengths/Å					
N_1C_2		1.320	1.339	1.329	1.346	1.328	1.346	1.331	1.348
		(1.321)	(1.340)	(1.330)	(1.347)	(1.329)	(1.347)	(1.332)	(1.350)
C_2C_3		1.384	1.394	1.378	1.388	1.377	1.387	1.375	1.386
		(1.386)	(1.396)	(1.379)	(1.389)	(1.379)	(1.389)	(1.379)	(1.388)
C_3C_4		1.390	1.403	1.391	1.404	1.392	1.404	1.393	1.405
		(1.391)	(1.403)	(1.392)	(1.405)	(1.392)	(1.405)	(1.392)	(1.405)
$C_4C_{4'}$	1.47	1.488	1.484	1.488	1.483	1.488	1.483	1.487	1.482
		(1.489)	(1.485)	(1.489)	(1.484)	(1.488)	(1.484)	(1.488)	(1.483)
Al_IN_1				2.004	2.003	2.043	2.027	1.970	1.971
				(1.999)	(1.997)	(2.046)	(2.034)	(1.965)	(1.966)
				Dihedral Angle/deg					
$C_3C_4C_{4'}C_{5'}$ (ω)	37.2	43.7	36.3	44.4	37.0	44.6	37.4	44.2	36.5
		(44.6)	(38.0)	(45.1)	(39.0)	(45.3)	(38.9)	(44.9)	(37.7)

[a] Only the bond lengths of the bound pyridyl ring of 44BPY in the complexes are given. [b] Reference 57.

TABLE 4: AlO Bond Lengths in the Alumina Clusters and in Their Lewis Complexes with PY and 44BPY Optimized at HF and B3LYP Levels with the 6-31G* and 6-31+G* (in Brackets) Basis Sets

	Al_IO_I[a]/Å		$Al_{II}O_I$/Å		$Al_{II}O_{II}$/Å		$Al_{III}O_{II}$/Å		$Al_{III}O_{III}$/Å	
	HF	B3LYP	HF	B3LYP	HF	B3LYP	HF	B3LYP	HF	B3LYP
$Al(OH)_3$	1.683	1.706								
	(1.678)	(1.701)								
$PY/Al(OH)_3$	1.730	1.745								
	(1.732)	(1.750)								
$44BPY/Al(OH)_3$	1.729	1.745								
	(1.732)	(1.750)								
$Al_4O_9H_6$	1.681	1.694	1.682	1.699	1.689	1.706				
	(1.681)	(1.697)	(1.682)	(1.701)	(1.690)	(1.710)				
$PY/Al_4O_9H_6$	1.716	1.729	1.670	1.688	1.696	1.713				
	(1.716)	(1.731)	(1.669)	(1.688)	(1.697)	(1.717)				
$44BPY/Al_4O_9H_6$	1.716	1.729	1.670	1.688	1.695	1.713				
	(1.716)	(1.731)	(1.669)	(1.689)	(1.697)	(1.717)				
$Al_{10}O_{21}H_{12}$	1.733	1.750	1.742	1.765	1.664	1.680	1.701	1.722	1.695	1.714
	(1.735)	(1.757)	(1.736)	(1.761)	(1.664)	(1.681)	(1.697)	(1.719)	(1.695)	(1.716)
$PY/Al_{10}O_{21}H_{12}$	1.776	1.790	1.729	1.750	1.668	1.684	1.700	1.721	1.700	1.719
	(1.780)	(1.800)	(1.724)	(1.747)	(1.667)	(1.685)	(1.697)	(1.718)	(1.700)	(1.721)
Al_4O_6	1.722	1.744	1.722	1.744	1.722	1.744				
	(1.722)	(1.746)	(1.722)	(1.746)	(1.722)	(1.746)				
PY/Al_4O_6	1.762	1.781	1.704	1.727	1.725	1.747				
	(1.762)	(1.781)	(1.704)	(1.728)	(1.725)	(1.749)				
$44BPY/Al_4O_6$	1.761	1.781	1.705	1.727	1.725	1.747				
	(1.761)	(1.782)	(1.704)	(1.728)	(1.725)	(1.749)				

[a] Experimental value: 1.72 Å in ref 64.

and 44BPY on the different cluster models determined at the B3LYP/6-31+G* level are shown in Figure 1.

1. Free PY and 44BPY and Free Clusters. Various experimental[57,86] and recent theoretical studies[55,56,87,88] on 44BPY have been made, often mainly concerned with the determination of the rotational conformation of the two pyridyl rings around the inter-ring bond, represented by the dihedral angle $C_3C_4C_{4'}C_{5'}$ (ω). According to previous calculations at the HF and B3LYP levels with 6-31G(+*) basis set,[56] we have concluded that 44BPY can be described by two aromatic rings linked by a single bond in a nonplanar conformation (D_2 symmetry). The present calculations (Table 3) are very close. The inter-ring bond $C_4C_{4'}$ and the rotation angle ω are in better agreement with experiment[57] when calculated with the B3LYP method than with the HF method.

The molecular structure of PY has been determined in the gas phase[58,59] and largely investigated by quantum chemistry methods.[60−63,81] Our B3LYP calculations (Table 2) very ac-

TABLE 5: Charges Transferred from PY or 44BPY to the Alumina Clusters upon Adsorption Determined by ESP at HF and B3LYP Levels Using the 6-31G* and 6-31+G* (in Brackets) Basis Sets

	HF			B3LYP		
complexes	unbound ring	bound ring	alumina	unbound ring	bound ring	alumina
PY/$Al(OH)_3$		0.420	−0.420		0.452	−0.452
		(0.428)	(−0.428)		(0.463)	(−0.463)
44BPY/$Al(OH)_3$	0.039	0.380	−0.419	0.048	0.402	−0.450
	(0.038)	(0.389)	(−0.427)	(0.044)	(0.417)	(−0.461)
PY/$Al_4O_9H_6$		0.231	−0.231		0.289	−0.289
		(0.199)	(−0.199)		(0.225)	(−0.225)
44BPY/$Al_4O_9H_6$	0.037	0.193	−0.230	0.055	0.231	−0.286
	(0.028)	(0.166)	(−0.194)	(0.048)	(0.169)	(−0.217)
PY/$Al_{10}O_{21}H_{12}$		0.252	−0.252		0.308	−0.308
		(0.221)	(−0.221)		(0.245)	(−0.245)
PY/Al_4O_6		0.628	−0.628		0.662	−0.662
		(0.605)	(−0.605)		(0.641)	(−0.641)
44BPY/Al_4O_6	0.062	0.561	−0.622	0.086	0.575	−0.661
	(0.059)	(0.538)	(−0.598)	(0.082)	(0.552)	(−0.634)

curately reproduce the experimental data.[58] Whatever the method considered, PY is characterized by an aromatic ring (C_{2v} symmetry).

In the two hydrogenated clusters $Al(OH)_3$ and $Al_4O_9H_6$, the length of the Al_IO_I surface bond (Table 4) is underestimated by ∼0.04 Å at the HF level and by a smaller value of ∼0.02 Å at the B3LYP level with respect to the Al−O experimental value of 1.72 Å derived from X-ray experiment.[64] Whereas, in the larger hydrogenated cluster $Al_{10}O_{21}H_{12}$, the Al_IO_I is overestimated by 0.015 Å at the HF level and by a larger value of 0.037 Å at the B3LYP level. In the non-hydrogenated cluster Al_4O_6, the Al_IO_I bond is more accurately calculated: at B3LYP level, it is overestimated by 0.02 Å and by only 0.002 Å at the HF level.

2. Lewis Complexes of PY and 44BPY with Alumina Clusters. Whatever the method applied, it is found that the diffuse functions in the 6-31+G* basis set have no effect on the structures for all species considered in this study (molecules, clusters, and complexes). The largest deviation of 0.007 Å arises at the B3LYP level between the two basis sets 6-31G* and 6-31+G* for Al_IN_1 intermolecular distance. In the following, we generally focus our attention on the calculation results obtained at the B3LYP/6-31+G* level.

Whatever the cluster considered, PY and 44BPY are adsorbed in a similar way on the surface Lewis acid site (Al^{3+}) of alumina. The interaction between 44BPY and Al^{3+} is monodentate, as for PY, via the nitrogen atom of only one of the two pyridyl rings. The pyridyl ring bound to the surface is perpendicular to the plane of the O_I atoms. In the Lewis complexes, the geometrical structure of the pyridyl ring of 44BPY nonimplicated in the adsorption, the inter-ring bond $C_4C_{4'}$ and the rotation angle ω are not changed. On the other hand, the structural parameters of PY and of the pyridyl ring (of the 44BPY molecule) involved in the interaction are modified. The structural modifications are principally localized in the nitrogen region. At all levels of calculation, the N_1C_2 and C_6N_1 bonds are longer after the complexation by ∼0.009 Å. The C_2C_3 and C_5C_6 bonds parallel to the N_1Al_I axis are shortened by ∼0.007 Å. The C_3C_4 and C_4C_5 bonds, far from the interaction region, are only slightly lengthened by less than 0.002 Å. These geometric modifications result from quaternisation of the ring upon interaction of the nitrogen atom of PY or 44BPY with the Al^{3+} surface Lewis acid site of alumina. They do not depend on the cluster size. This confirms the local character of the adsorption.

Upon the adsorption, the coordination of the Al_I^{3+} surface Lewis acid site involved in the interaction passes from 3 to 4, so the structure around the Al_I atom becomes tetragonal during the formation of the Al_IN_1 intermolecular bond. As shown in Table 4, at all levels of calculation, the Al_IO_I bonds in the four alumina clusters lengthen by ∼0.04 Å, the $Al_{II}O_I$ bonds become shorter with average shifts of 0.012, 0.013, and 0.018 Å for Lewis complexes with $Al_4O_9H_6$, $Al_{10}O_{21}H_{12}$, and Al_4O_6 clusters, respectively, whereas, the terminal AlO bonds remain approximately unchanged in length.

The Al_IN_1 intermolecular distance should be theoretically related to the strength of the Lewis acid sites: the shorter the Al_IN_1 distance is, the stronger the Lewis acid site is. Whatever the calculation method used, the Al_IN_1 intermolecular bond lengths for PY and 44BPY into a given Lewis complex have nearly the same values (Tables 2 and 3). On the other hand, they are sensitive to the size and to the shape of the alumina cluster. Thus, the Al_IN_1 bond lengths increase in the order Al_4O_6 < $Al(OH)_3$ < $Al_4O_9H_6$ < $Al_{10}O_{21}H_{12}$. This indicates that Al_4O_6 is a much stronger Lewis acid than the hydrogenated clusters. In the case of the interaction of PY or 44BPY with the three hydrogenated clusters, it is surprising to find that at all levels of calculation, the Al_IN_1 distances in the complexes formed with the small cluster $Al(OH)_3$ are shorter than those in the complexes formed with $Al_4O_9H_6$ and $Al_{10}O_{21}H_{12}$ clusters. This difference is probably caused by a steric hindrance between PY or 44BPY and surface oxygen ions in $Al_4O_9H_6$ and $Al_{10}O_{21}H_{12}$ clusters.

B. Charge Transfer. The net intermolecular charge transfers determined at different levels of calculation by the electrostatic potential analysis (ESP) are given in Table 5. Table 5 shows the ESP charges transferred from PY and 44BPY ligands to alumina clusters upon adsorption estimated at the HF and B3LYP levels using both 6-31G* and 6-31+G* basis sets. Their values are slightly sensitive to the correlation effect. Thus, in all cases, the HF values are slightly smaller than those determined at the B3LYP level with the same basis set. Comparison of both basis sets 6-31G* and 6-31+G* shows that the effect of diffuse functions, except for $Al_4O_9H_6$, does not lead to significant changes in the intermolecular charge-transfer values. On the other hand, whatever the basis set, for PY and 44BPY complexes formed with the hydrogenated clusters, the ESP charges determined at both levels HF and B3LYP depend on the cluster size.

The ESP analysis of charges in free alumina clusters and their complexes with PY and 44BPY ligands suggests that the non-hydrogenated cluster Al_4O_6 and its complexes are very strongly ionic in character, with respect to the complexes formed with the hydrogenated clusters. Thus, this interaction is mainly electrostatic in nature and yields to the formation of the strongly bound charge-transfer complexes. As shown in Table 5, at all

TABLE 6: Adsorption Energies (kcal/mol) of PY and 44BPY Ligands Adsorbed on the Lewis Acid Sites of the Different Alumina Clusters $Al(OH)_3$, $Al_4O_9H_6$, $Al_{10}O_{21}H_{21}$, and Al_4O_6, Calculated at HF and B3LYP Levels Using the 6-31G* and 6-31+G* (in Brackets) Basis Sets, Uncorrected (ADE_{un}) and Corrected (ADE_c) for Zero Point Energy (ZPE) and Basis Set Superposition Error (BSSE)

	HF				B3LYP			
complexes	ADE_{un}	ZPE	BSSE	ADE_c	ADE_{un}	ZPE	BSSE	ADE_c
$PY/Al(OH)_3$	−37.8	2.6	4.4	−30.8	−38.7	2.2	5.9	−30.6
	(−35.9)	(2.7)	(2.0)	(−31.2)	(−36.5)	(2.4)	(2.0)	(−32.1)
$44BPY/Al(OH)_3$	−37.4	2.5	4.4	−30.5	−38.6	2.1	6.1	−30.4
	(−35.6)	(2.6)	(2.2)	(−30.8)	(−36.2)	(2.1)	(2.1)	(−32.0)
$PY/Al_4O_9H_6$	−29.5	1.7	4.9	−22.9	−32.4	1.6	6.3	−24.5
	(−26.7)	(0.9)	(2.8)	(−23.0)	(−28.3)	(1.4)	(2.5)	(−24.4)
$44BPY/Al_4O_9H_6$	−28.6	1.5	4.9	−22.2	−31.8	1.4	6.2	−24.2
	(−26.2)	(1.4)	(3.1)	(−21.7)	(−27.8)	(1.1)	(2.7)	(−24.0)
$PY/Al_{10}O_{21}H_{12}$	−35.9	2.1	7.8	−26.0	−39.3	2.4	9.8	−27.1
	(−31.1)	(2.1)*	(4.8)	(−24.2)	(−31.9)	(2.4)*	(4.2)	(25.3)
PY/Al_4O_6	−51.9	1.6	3.8	−46.5	−51.9	1.7	5.1	−45.1
	(−51.1)	(1.6)	(2.6)	(−47.0)	(−49.9)	(1.7)	(2.2)	(−46.0)
$44BPY/Al_4O_6$	−51.1	1.4	3.6	−46.1	−51.2	1.5	4.8	−44.9
	(−50.8)	(1.4)	(2.8)	(−46.6)	(−49.6)	(1.5)	(2.4)	(−45.7)

levels of calculation, the ESP charges transferred from PY or 44BPY to the clusters increase in the same order of the adsorption energies (as it will be shown in the next section): $Al_4O_9H_6 < Al_{10}O_{21}H_{12} < Al(OH)_3 < Al_4O_6$.

In all complexes, both PY and 44BPY ligands have nearly the same charge transfer values (Table 5). However, the charge transferred from the ligand to the alumina cluster is very slightly larger with PY than with 44BPY. This charge transferred from the ligand to the alumina cluster produces an electrostatic attraction that dominates the bonding. It is obviously normal that the electron distribution of the pyridyl ring of the 44BPY molecule that binds to the surface will be considerably more perturbed than that of the ring that is not bound to the surface. Thus, the major charge transfer in these complexes occurs between the bound pyridyl ring and the alumina cluster. In fact, the amount of charge of the unbound pyridyl ring changes very little upon complexation; by less than 0.09 of an electron (Table 5). The most noticeable consequences of the explicit exclusion of hydrogen atom in the Al_4O_6 model are a strongly larger adsorption energy for both ligands PY and 44BPY and a larger charge transfer from the nitrogen atom of the ligands to the Al Lewis acid site of the Al_4O_6 cluster.

C. Energetics. The adsorption energies with and without ZPE and BSSE corrections (ADE_c and ADE_{un}) for the interaction of PY and 44BPY ligands via the N lone pair with the Al Lewis acid sites of the four clusters $Al(OH)_3$, Al_4O_6, $Al_4O_9H_6$, and $Al_{10}O_{21}H_{12}$ are shown in Table 6. In all cases, the ZPE contributions to the adsorption energies are very small and range from 0.9 to 2.7 kcal/mol. Whatever the method of calculation and the basis set used, the BSSE corrections are proportionally more significant for PY and 44BPY complexes formed with the hydrogenated clusters, which increase with the size of the cluster, than for complexes formed with non-hydrogenated cluster.

Without the diffuse functions using the 6-31G* basis set, it is surprising that BSSE calculated for all complexes at the B3LYP level (4.8−9.8 kcal/mol) are larger than those estimated at the HF level (3.6−7.8 kcal/mol). At the B3LYP/6-31G* level, the BSSE corrections represent less than 10% of ADE_{un} for complexes formed with Al_4O_6. Whereas, they represent 15%, 19%, and 24% of ADE_{un} for complexes formed with $Al(OH)_3$, $Al_4O_9H_6$, and $Al_{10}O_{21}H_{12}$ clusters, respectively. This indicates that the 6-31G* basis set is less adapted for complexes formed with the hydrogenated clusters than for complexes formed with the non-hydrogenated cluster.

It is found that diffuse functions are important to reduce the BSSE correction. With the 6-31+G* including diffuse functions, the BSSE errors calculated at the B3LYP level are slightly lower than those estimated at the HF level. Except for $PY/Al_{10}O_{21}H_{12}$ complex (its BSSE represents 13% of ADE_{un} at the B3LYP/6-31+G* level), the BSSE corrections estimated at the B3LYP/6-31+G* level represent less than 10% of ADE_{un}.

The inclusion of electron correlation via B3LYP approach has a slight effect on ADE_{un} values. Even when ZPE and BSSE corrections are included, the theoretically predicted values of adsorption energies for all complexes are not very dependent on the methods applied. For adsorption energies computed using the 6-31+G* basis set, the largest deviation of 2.3 kcal/mol arises between HF and B3LYP data for the $44BPY/Al_4O_9H_6$ complex.

Whatever the method of calculation and the basis set used, the adsorption energies of PY and 44BPY molecules adsorbed on Al_4O_6 cluster (∼46 kcal/mol) compare very well to the experimental value of ∼45 kcal/mol for ammonia adsorption on alumina surface.[92] They are considerably larger than those obtained with $Al(OH)_3$ (∼32 kcal/mol), $Al_4O_9H_6$ (∼24 kcal/mol), and $Al_{10}O_{21}H_{12}$ (∼25 kcal/mol). It should be noted that others experimental values range from 20 to 40 kcal/mol.[93] However, the Al_4O_6 cluster is more adapted to represent the ionic character of alumina surface than the hydrogenated clusters.

Although the $Al_4O_9H_6$ and $Al_{10}O_{21}H_{12}$ clusters are larger than Al_4O_6, the PY and 44BPY complexes formed with the Al_4O_6 cluster are more strongly bound than those formed with both hydrogenated clusters. This is explained by the larger ionicity of Al_4O_6 with respect to the hydrogenated clusters

In the case of the interaction of PY or 44BPY with the hydrogenated clusters, it is surprising to find that, at all levels of calculation, the adsorption energies of PY and 44BPY adsorbed on the small $Al(OH)_3$ cluster (∼31 kcal/mol) are larger than those adsorbed on larger $Al_4O_9H_6$ and $Al_{10}O_{21}H_{12}$ clusters (∼25 kcal/mol). This difference is caused by a steric hindrance between PY or 44BPY and surface oxygen ions in $Al_4O_9H_6$ and $Al_{10}O_{21}H_{12}$ clusters.

On the basis of these results, we conclude that the adsorption energies of PY and 44BPY adsorbed on Al Lewis acid sites in alumina clusters depend more on the ionic character of the cluster model than on its size.

Irrespective of the cluster model considered and the method of calculation used, the adsorption energies of PY are slightly larger than those of 44BPY by less than 1.3 kcal/mol. This suggests that the molecule-surface interaction is essentially localized between the nearest pyridyl ring of 44BPY to the

TABLE 7: Scaled Frequencies (cm^{-1}) of PY and Its Lewis Complexes in the 950−1650 cm^{-1} Region with Alumina Clusters Determined at HF (in Italics) and B3LYP Levels with the 6-31+G* Basis Set[l]

		PY			PY/alumina	PY/$Al(OH)_3$		PY/$Al_4O_9H_6$		PY/$Al_{10}O_{21}H_{12}$[i]		PY/Al_4O_6	
approximate description[a,b]		ν_{exp}[c]	ν_{B3LYP}[d] PED[e]	ν_{HF}[d]	ν_{exp}[f] ($\Delta\nu$)[g]	ν_{B3LYP}[d] ($\Delta\nu$)[g]	ν_{HF}[d] ($\Delta\nu$)[g]	ν_{B3LYP}[d] ($\Delta\nu$)[g]	ν_{HF}[d] ($\Delta\nu$)[g]	ν_{B3LYP}[j] ($\Delta\nu$)[k]	ν_{HF}[j] ($\Delta\nu$)[k]	ν_{B3LYP}[d] ($\Delta\nu$)[g] PED[e]	ν_{HF}[d] ($\Delta\nu$)[g]
$\nu_{CC}+\delta_r$	**(1-A_1)**	**991**	**986** $S_1(55),R_1(27),R_2(12)$	***983***	**1019**[h] (+28)	**1015** (+29)	**1002** *(+19)*	**1016** (+30)	**1001** *(+18)*	**1013** (+30)	**999** *(+19)*	**1013** (+27) $R_3(38),R_2(25),R_1(12),S_1(11)$	**1001** *(+19)*
$\delta_r+\nu_{CC}$	**(12-A_1)**	**1032**	**1021** $S_1(35),R_3(31),R_2(19)$	***1009***	**1045**[h] (+13)	**1040** (+19)	**1033** *(+25)*	**1037** (+16)	**1030** *(+21)*	**1034** (+13)	**1031** *(+25)*	**1042** (+21) $S_1(81)$	**1035** *(+26)*
ν_{CC}	**(19b-B_2)**	**1442**	**1447** $R_2(27),\beta_3(25),\beta_4(19),\beta_2(15),R_1(10)$	***1446***	**1452** (+10)	**1457** (+10)	**1454** *(+8)*	**1456** (+9)	**1455** *(+8)*	**1458** (+10)	**1454** *(+10)*	**1458** (+11) $R_2(34),\beta_3(23),\beta_2(17),\beta_4(15)$	**1455** *(+9)*
ν_{CC}	**(19a-A_1)**	**1483**	**1485** $\beta_2(46),\beta_3(28),R_1(18),R_3(15)$	***1490***	**1495** (+12)	**1493** (+8)	**1497** *(+6)*	**1494** (+9)	**1500** *(+9)*	**1501** (+15)	**1503** *(+15)*	**1493** (+8) $\beta_2(38),\beta_3(34),R_3(20),R_1(14)$	**1497** *(+6)*
ν_{CC}	**(8b-B_2)**	**1581**	**1590** $R_3(54),R_1(27),\beta_4(15),S_3(12)$	***1606***	**1577** (−4)	**1586** (−4)	**1601** ***(−5)***	**1588** (−1)	**1605** *(−1)*	**1586** (−5)	**1602** *(−3)*	**1584** (−6) $R_3(57),R_1(27),\beta_4(16),S_3(11)$	**1599** *(−7)*
ν_{CC}	**(8a-A_1)**	**1590**	**1595** $R_2(52),R_3(16),\beta_3(15),\beta_2(13),R_1(13),S_2(10)$	***1616***	**1623** (+33)	**1627** (+31)	**1641** *(+25)*	**1626** (+30)	**1641** *(+25)*	**1626** (+28)	**1640** *(+24)*	**1627** (+31) $R_2(52),\beta_2(19),R_3(16),R_1(12),S_2(11),\beta_3(10)$	**1640** *(+25)*

[a] Assignments with Wilson notation are given in brackets. [b] C_{2v} symmetry. [c] Reference 75. [d] The scaling factors are ∼0.974 and ∼0.901 for B3LYP and HF frequencies, respectively. [e] PED are expressed in %; values lower than 10% are neglected. [f] IR frequencies (cf text). [g] $\Delta\nu$ is the frequency shift relative to the PY value. [h] Raman frequency in ref 18. [i] Frequencies calculated with the 6-31G* basis set. [j] The scaling factors are ∼0.972 and ∼0.897 for B3LYP and HF frequencies, respectively. [k] $\Delta\nu$ is the frequency shift relative to the PY value calculated with the 6-31G* basis set. [l] Available experimental values are given for comparison.

surface and the Al Lewis acid site of this surface. The slightly larger stability of PY complexes would be expected, owing to the greater basicity of PY with respect to 44BPY.[26]

The influence of the rotation of an adsorbed species around the Al_lN_1 axis was studied for σ bonding of PY complexed with the Al Lewis acid site of each cluster model. No pronounced dependence of this rotation on the total energy of the adsorption complex is found (less than 1.0 kcal/mol).

It should be noted that for PY/Al_4O_6 the possibility of the formation of a π adsorption complex, corresponding to the interaction between the Al Lewis acid site and the pyridine π-system, was examined at the HF and B3LYP levels with the 6-31G* basis set. A local minimum corresponding to the π structure is found on the potential energy surface. However, the π complex is strongly less stable than the σ complex by ∼34.2 kcal/mol.

Finally, some calculations for PY/$Al(OH)_3$ complex were performed at the MP2 and MP4 levels with the 6-31+G* basis set in order to test the results of B3LYP approach. We found an adsorption energy of 34.0 and 33.8 kcal/mol, respectively, compared to 32.1 kcal/mol obtained at the B3LYP/6-31+G* level.

D. Vibrational Properties. Although results of energy and frequency calculations are complementary in our study, the frequency analysis is used to check the adequacy of these models, which is important for their further employment in studying the adsorption on alumina. The computed frequencies and frequency shifts in the 750−1700 cm^{-1} spectral region for PY and 44BPY ligands adsorbed on the four cluster models are shown in Tables 7 and 8 together with the appropriate literature data. Detailed examination of our results shows that computed frequency shifts are significantly less sensitive to the cluster size, diffuse functions, and correlation effects than the computed adsorption energy.

1. Free and Adsorbed PY. For the free pyridine molecule (C_{2v} symmetry), the 27 vibrational modes are shared among $10A_1 + 3A_2 + 5B_1 + 9B_2$ symmetry classes. Adsorption on the alumina surface of PY via its nitrogen atom does not affect the molecular symmetry of the pyridyl ring. All vibrational modes of PY are Raman active, and only the A_1, B_1, and B_2 modes of vibration are IR active.

As mentioned above, the two ring stretching modes 8a (a_1 symmetry) and 19b (a_2 symmetry) of pyridine observed in the 1400−1700 cm^{-1} region are the most affected modes upon adsorption. Morterra et al.[12] described three different Lewis acid sites on α- and η-Al_2O_3 surface characterized by three different frequency ranges of 8a mode at 1626−1620 cm^{-1} (site I), 1618−1612 cm^{-1} (site II), and 1600−1590 cm^{-1} (site III). Site I corresponds to coordinately unsaturated tetrahedral Al^{3+} cations, site II is related to a pair of coordinately unsaturated Al^{3+} cations in octahedral and tetrahedral coordination, and site III is assigned to coordinately unsaturated octahedral Al^{3+} cations. Parry[15] and Pichat et al.[23] have reported that the frequencies of the other vibrational modes 19a (a_1 symmetry) and 8b (b_2 symmetry) observed in the 1400−1700 cm^{-1} region also increase.

Hendra et al.[18] have investigated the Raman spectra of pyridine over alumina. He demonstrated that the skeletal motions near 1000 cm^{-1}, i.e., the in-plane deformation 12 mode (a_1 symmetry) and the breathing 1 mode (a_1 symmetry), allow also the differentiation of Lewis and Brönsted acid sites. In particular, the greater the coordinate interaction between the nitrogen of PY and the metal atom of the surface is, the more the frequency of the mode 1 is shifted.

Therefore, the comparison between experimental and calculated frequencies is limited to these six modes.

Harmonic vibrational frequencies calculated at the HF and B3LYP are usually systematically larger than the corresponding experimental values. They can be corrected by emperical scaling factors,[65] calculated from the mean deviation of the computed frequencies from the experimental values of PY. Scaling factors of ∼0.901 and ∼0.974 have been determined with the 6-31+G*

TABLE 8: Scaled Frequencies (cm^{-1}) of 44BPY and Its Lewis Complexes with Alumina Clusters in the 700−1700 cm^{-1} Region Determined at HF (in Italics) and B3LYP Levels with the 6-31+G* Basis Set[h]

approximate description[a,b]		44BPY			44BPY/alumine	44BPY/Al(OH)$_3$		44BPY/Al$_4$O$_9$H$_6$		44BPY/Al$_4$O$_6$	
		ν_{exp}[c]	ν_{B3LYP}[d] PED[e]	ν_{HF}[d]	ν_{exp}[f] ($\Delta\nu$)[g]	ν_{B3LYP}[d] ($\Delta\nu$)[g]	ν_{HF}[d] ($\Delta\nu$)[g]	ν_{B3LYP}[d] ($\Delta\nu$)[g]	ν_{HF}[d] ($\Delta\nu$)[g]	ν_{B3LYP}[d] ($\Delta\nu$)[g] PED[e]	ν_{HF}[d] ($\Delta\nu$)[g]
$\delta_r+\nu_{NC}+\nu_{ir}$	(1-*A*)	**756**	**746** $S_2(49),R_3(21),$ $R(17),S_1(10)$	***735***		**765** (+19)	**753** *(+19)*	**766** (+20)	**751** *(+16)*	**767** (+21) $S_2(31),S'_2(15),$ $R(14),R_3(12),$ $R'_3(9),S'_1(5)$	**755** *(+21)*
$\delta_r+\nu_{CC}$	(1-B_1)	**1038**	**1031** $S_1(42),R_3(26),$ $R_2(19)$	***1019***	**1045** (+7)	**1037** (+7)	**1029** *(+10)*	**1037** (+6)	**1029** *(+10)*	**1039** (+8) $S_1(77)$	**1031** *(+12)*
$\beta_{CH}+\nu_{CC}$	(18b-B_3)	**1075**	**1091** $\beta_3(38),R_2(36),$ $\beta_2(13)$	***1055***	**1067** (−8)	**1092** (+1)	**1055** *(0)*	**1093** (+2)	**1055** *(0)*	**1094** (+3) $R'_2(38),\beta'_3(31),$ $\beta'_2(14)$	**1054** *(−1)*
$\beta_{CH}+\nu_{CC}$	(18b-B_2)	**1082**	**1093** $R_2(35),\beta_3(25),$ $\beta_2(16)$	***1061***	**1075** (−7)	**1110** (+18)	**1081** *(+20)*	**1110** (+17)	**1085** *(+24)*	**1112** (+19) $\beta_3(30),R_2(27),$ $\beta_2(19),R_1(10)$	**1088** *(+27)*
$\beta_{CH}+\nu_{NC}$	(9a-B_1)	**1218**	**1222** $\beta_2(38),\beta_3(20),$ $R_1(17)$	***1213***	**1218** (0)	**1223** (+2)	**1215** ***(+2)***	**1222** (0)	**1215** *(2)*	**1223** (+1) $\beta_2(24),\beta_3(17),$ $\beta'_2(12),R_1(9),$ $R_2(7),R'_1(6),$ $\beta'_3(6)$	**1215** *(+2)*
$\beta_{CH}+\nu_{NC}$	(9a-*A*)	**1219**	**1226** $\beta_2(35),\beta_3(23),$ $R_1(15)$	***1215***	**1225** (+6)	**1228** (+2)	**1220** *(+5)*	**1224** (−2)	**1217** *(2)*	**1227** (+1) $\beta'_2(24),\beta'_3(16),$ $R'_1(10),\beta_2(10),$ $\beta_3(9),R'_2(5)$	**1219** *(+4)*
β_{CH}	(3,9b,15-B_2)	**1324**	**1325** $\beta_3(51),R_2(19),$ $R_1(18),\beta_2(17)$	***1314***	**1319** (−5)	**1326** (+1)	**1317** *(+3)*	**1327** (+2)	**1318** *(+4)*	**1327** (+2) $\beta_3(26),\beta'_3(22),$ $\beta_2(13),R_1(13),$ $R_2(10),R'_2(8),$ $\beta'_2(7),R'_1(7)$	**1318** *(+4)*
β_{CH}	(3,9b,15-B_3)	**1344**	**1339** $\beta_2(44),\beta_3(42),$ $\beta_4(8)$	***1335***		**1340** (+1)	**1339** **(+4)**	**1338** (−1)	**1339** *(+4)*	**1341** (+2) $\beta'_3(24),\beta'_2(24),$ $\beta_2(21),\beta_3(18)$	**1339** *(+5)*
$\beta_{CH}+\nu_{CC}$	(19b-B_2)	**1406**	**1410** $\beta_2(62),R_2(34)$	***1400***	**1407** (+1)	**1413** (+3)	**1406** *(+6)*	**1416** (+6)	**1407** *(+6)*	**1414** (+4) $\beta'_2(49),R'_2(30),$ $\beta'_3(11),\beta_2(6)$	**1406** *(+6)*
$\beta_{CH}+\nu_{CC}$	(19b-B_3)	**1424**	**1420** $\beta_2(37),R_2(32),$ $\beta_3(19)$	***1414***	**1448** (+24)	**1435** (+15)	**1427** *(+13)*	**1432** (+12)	**1425** *(+10)*	**1438** (+18) $R_2(42),\beta_2(38),$ $\beta_3(14)$	**1429** *(+15)*
$\beta_{CH}+\nu_{CC}$	(19a-B_1)	**1487**	**1489** $\beta_2(47),\beta_3(27),$ $R_1(20),R_3(14)$	***1493***	**1488** (+1)	**1492** (+3)	**1497** *(+4)*	**1495** (+6)	**1499** *(+6)*	**1492** (+3) $\beta'_2(31),\beta'_3(17),$ $\beta_2(14),R'_1(13),$ $\beta_3(12),R'_3(9)$	**1497** *(+4)*
$\beta_{CH}+\nu_{CC}$	(19a-*A*)	**1511**	**1509** $\beta_2(45),R_1(22),$ $\beta_3(18),R_3(14),$ $R(9)$	***1519***	**1510** (−1)	**1517** (+8)	**1525** *(+6)*	**1517** (+8)	**1527** *(+8)*	**1517** (+8) $\beta_2(23),\beta_3(17),$ $\beta'_2(16),R_3(14),$ $R(11),R_1(10),$ $R'_1(8)$	**1525** *(+6)*
ν_{CC}	(8b-B_2)	**1531**	**1547** $R_3(45),R_1(40),$ $S_3(13),\beta_3(10)$	***1565***	**1535** (+4)	**1544** (−3)	**1562** *(−3)*	**1544** (−3)	**1564** *(−1)*	**1543** (−4) $R_3(33),R_1(25),$ $R'_1(14),R'_3(14),$ $S_3(9)$	**1559** *(−6)*
ν_{CC}	(8a-B_1)	**1589**	**1600** $R_2(52),R_3(17),$ $\beta_3(17),R_1(12),$ $\beta_2(12),S_2(11)$	***1614***		**1602** (+2)	**1621** *(+7)*	**1604** (+4)	**1623** *(+9)*	**1602** (+2) $R'_2(48),R'_3(20),$ $\beta'_3(18),S'_2(11),$ $\beta'_2(10),R'_1(10)$	**1621** *(+7)*
ν_{CC}	(8b-B_3)	**1596**	**1576** $R_3(53),R_1(31),$ $S_3(13),\beta_3(10)$	***1593***	**1600** (+4)	**1574** (−2)	**1591** *(−2)*	**1576** (0)	**1594** *(+1)*	**1574** (−2) $R'_3(36),R'_1(22),$ $R_3(18),R_1(9),$ $S'_3(9),\beta'_4(6),$ $\beta'_2(5),\beta_4(6)$	**1591** *(−2)*
ν_{CC}	(8a-*A*)	**1607**	**1607** $R_2(44),R_3(23),$ $\beta_3(19),S_2(12),$ $R(10)$	***1633***	**1630** (+23)	**1633** (+26)	**1649** *(+16)*	**1633** (+27)	**1648** *(+15)*	**1634** (+27) $R_2(51),\beta_2(17),$ $R_3(14),R_1(13),$ $\beta_3(12),S_2(11)$	**1648** *(+15)*

[a] Assignments with Wilson notation in brackets. [b] D_2 symmetry. [c] Reference 56. [d] The scaling factors are ∼0.975 and ∼0.899 for B3LYP and HF frequencies, respectively. [e] PED are expressed in %; values lower than 5% are neglected. [f] IR frequencies in ref 26. [g] $\Delta\nu$ is the frequency shift relative to the 44BPY value. [h] Available experimental values are given for comparison.

basis set at the HF and B3LYP levels, respectively. Without the diffuse functions using the 6-31G* basis set, they are slightly smaller (∼0.897 and ∼0.972 at the HF and B3LYP levels, respectively).

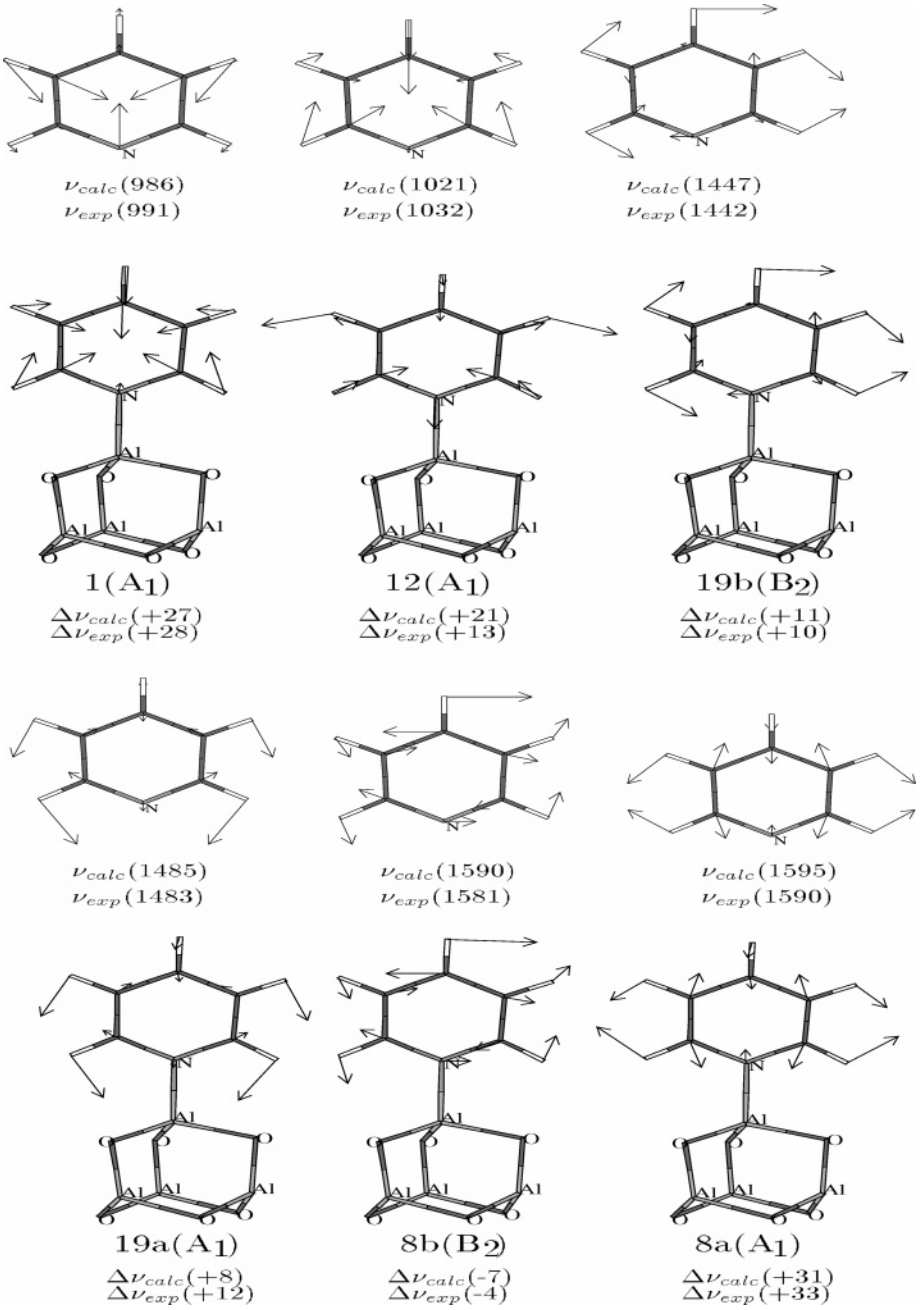

Figure 3. Calculated vibrational patterns of some in-plane normal modes of free and adsorbed PY on Al_4O_6 cluster in the 950−1650 cm^{-1} spectral region. Numbers indicate the observed and calculated frequencies and frequency shifts in cm^{-1}. The scale for the arrows (displacements) is arbitrary but common to all the normal modes.

The experimental and scaled calculated frequencies of the six modes of interest for the free PY and its Lewis complexes are listed in Table 7 and displayed in Figure 3. Pyridine vibrational spectra have been largely studied in the past, principally by Raman and IR spectrometry in the gaseous and liquid phases[69−77] and also by ab initio and force field methods.[60,63,78−81] Recent experimental pyridine fundamentals based on Raman vapor and gas-phase FT-IR measurements[75] are given in Table 7. The experimental frequencies of the ν_{CC} modes between 1400 and 1700 cm^{-1} of pyridine adsorbed on alumina are mean values from the most recent FT-IR Raman spectra available in the literature.[14,16,19,21] For mode 8a, the experimental frequency compared to the calculated value corresponds to site I related to coordinately unsaturated tetrahedral Al^{3+} cation. The experimental frequencies of modes 1 and 12 of PY over alumina have been obtained by Raman spectrometry.[18] For the calculated modes, only the PEDs of the free PY and of PY adsorbed on the non-hydrogenated cluster Al_4O_6 obtained with the B3LYP method are given. In fact, for free PY or PY adsorbed on a given cluster, the PEDs are quite similar whatever the theoretical method used; in the same way, with a given calculation method, the PEDs of adsorbed pyridine are quite identical whatever the cluster considered. The PEDs are expressed in terms of local symmetry coordinates (Table 1 and Figure 2). Only contributions greater than 10% are indicated. The experimental and theoretical frequency shifts on going from free PY to adsorbed PY are also reported in Table 7. The complete set of calculated vibrational frequencies are available on request.

As can be seen from Table 7, there is a very good agreement between the scaled calculated frequencies at the HF or B3LYP level and experimental values for free and adsorbed PY. With HF/6-31+G* and B3LYP/6-31+G* methods, the mean absolute errors are $\sim 13 \pm 10$ and $\sim 5 \pm 3$ cm^{-1}, respectively. The

frequency shifts on going from free PY to adsorbed PY are also very well computed, the mean deviations with respect to experiment being $\sim 6 \pm 4$ and $\sim 3 \pm 3$ cm^{-1} at the HF and B3LYP levels, respectively. Thus, the B3LYP results are obviously superior to the HF ones for the vibrational frequencies and the frequency shifts.

The very good agreement between calculations and experiment concerning not only the absolute frequencies but also the frequency shifts on passing from free PY to PY adsorbed onto alumina clusters indicates that the modifications of the force constants and energy potential redistributions among normal coordinates upon adsorption are correctly calculated. This strongly supports the optimized geometry determined for adsorbed PY with both theoretical methods.

Modes 8b and 19a present nearly the same PEDs in free PY than in adsorbed PY. The frequencies of these modes are only slightly shifted on going from PY to PY adsorbed onto alumina, except for the PY/$Al_{10}O_{21}H_{12}$ complex for which the shift is larger. This may be accounted for by the weak variations upon adsorption of the force constants relative to the majority of the coordinates involved in the PEDs of these modes (Table 8), as evidenced from Table 1S. As the N_1C_2 bond increases upon adsorption, we might expect downward shifts for both modes. However, as shown by Table 1S, the relative force constant is only slightly lowered in adsorbed PY with Al_4O_6 and even increases with $Al(OH)_3$ and $Al_4O_9H_6$. By comparison, the force constant shift related to the C_2C_3 bond is significantly larger, whereas the C_2C_3 bond lengthening is smaller than the N_1C_2 bond decreasing. This disparity shows that the correlations between the force constants and the relative bond lengths are not always straightforward. In the present case, the calculated internal force constant derives from an electronic potential which is disturbed by the modification of the electronic distribution in the vicinity of the nitrogen atom upon adsorption. Consequently, it might not only correspond to the interatomic force constant. The shifts computed for these two modes are in good agreement with the experimental shifts.

Modes 1, 12, 19b, and 8a undergo significant positive shifts on passing from free PY to adsorbed PY. The PEDs of modes 19b and 8a are nearly unchanged upon adsorption. For mode 19b, the calculated upward shift on going from free pyridine to adsorbed pyridine correctly reproduces the experimental one ($\Delta\nu_{exp} = 10$ cm^{-1}, $\Delta\nu_{calc}$ between 8 and 11 cm^{-1}). It may reflect the increase of the force constant related to the R_2 coordinate. For mode 8a, a significant positive frequency shift upon adsorption is calculated for this mode, in good agreement with experiment ($\Delta\nu_{exp} = 33$ cm^{-1}, $\Delta\nu_{calc}$ between 25 and 31 cm^{-1}). This reflects, as for mode 19b, the increase of the force constant $k(R_2,R_2)$. This important shift may be compared to those already observed upon quaternisation of the pyridyl ring, for example on going from pyridine to pyridinium (+47 cm^{-1})[89] or to *N*-methyl-pyridinium (+49 cm^{-1})[90] or from 44BPY to *N*,*N*′-diprotonated cation $44BPYH_2^{2+}$ (+44 cm^{-1})[56] or to *N*,*N*′-dihydro cation radical $44BPYH_2^{\bullet +}$ (+55 cm^{-1}).[55]

Modes 1 and 12 are characterized by a potential energy largely redistributed upon adsorption. The frequencies of both modes are significantly upward shifted on passing from PY to adsorbed PY. The large positive frequency shift of mode 1 may be explained by the increase of the R_2 coordinate contribution in the PED and the increase of the related force constant $k(R_2,R_2)$ for adsorbed PY. The less upward frequency shift of mode 1 may result from the drastic increase of the S_1 coordinate contribution in the PED and the increase, even slight, of the corresponding force constant $k(S_1,S_1)$ (Table 1S).

2. Free and Adsorbed 44BPY. For the free 44BPY molecule (D_2 twisted symmetry), the 54 vibrational modes are classified as $14A + 12B_1 + 14B_2 + 14B_3$ symmetry classes. All vibrational modes of 44BPY are Raman active, whereas only the B_1, B_2, and B_3 modes of vibration are IR active. Upon adsorption, the symmetry of adsorbed 44BPY is reduced from D_2 to C_2. The 54 modes are transformed in $26A + 28B$ symmetry species (A and B_1 become A, B_2 and B_3 become B). The Raman active A totally symmetric modes (D_2 symmetry) become IR active A modes (C_2 symmetry), and thus all vibrational modes of adsorbed 44BPY may be observed both in Raman and IR spectrometry.

Bagshaw and Cooney[24,26] have observed FT-IR spectra of 44BPY adsorbed on γ-alumina between 1000 and 1700 cm^{-1}. The observed bands are related to the in-phase and out-of-phase components (relative to the inter-ring bond) of 7 pyridyl in-plane vibrations and to the out-of-phase component of an eighth pyridyl in-plane vibration. The comparison between the calculated and experimental frequencies of free or adsorbed 44BPY bears only on these vibrations. The 1400−1700 cm^{-1} region contains the ring stretching vibrational modes. As for PY, it has been shown that this is the most sensitive spectral range to adsorption. The 1000−1400 cm^{-1} region includes the CH bending and the ring breathing vibrational modes.

The frequencies used to establish the scaling factors for free or adsorbed 44BPY correspond to vibrational modes of which the assignment must be certain. For 44BPY adsorbed on alumina, the features observed at 1067 and 1075 cm^{-1}, which are not unambiguously assigned, must not be taken into account. Hence, all of the scaling factors are determined from the 11 frequencies actually detected for adsorbed 44BPY.

For free or adsorbed 44BPY, scaling factors of ~0.899 with HF/6-31+G* method and ~0.975 with B3LYP/6-31+G* method are obtained. The observed and scaled frequencies for 44BPY and its Lewis complexes are reported in Table 8 and displayed in Figure 4. The IR and Raman spectra of crystalline 44BPY have been reported in the literature.[52−56] Table 8 contains our more recent experimental data.[56] Accurate assignments have been obtained by our previous ab initio and B3LYP calculations using 3-21G(+*) and 6-31G(+*) basis sets.[55,56] The vibrational frequencies of 44BPY adsorbed on alumina, observed by FT-IR spectrometry by Bagshaw and Cooney,[26] are listed in Table 8. Only the PEDs of free 44BPY and adsorbed 44BPY on Al_4O_6 are presented in Table 8. In the PEDs of adsorbed 44BPY, the contributions indicated by primes correspond to the unbound pyridyl ring, and those without a prime are related to the bound pyridyl ring. In the PEDs of free 44BPY, the contributions relative to each pyridyl ring are identical, and so the different components of the PEDs correspond to the sum of the contributions of both rings. The calculated and observed frequency shifts on passing from free 44BPY to adsorbed 44BPY are also indicated in Table 8. The whole set of computed frequencies may be requested.

For free or adsorbed 44BPY, the scaled frequencies are in very good agreement with experiment. The mean absolute errors are $\sim 12 \pm 9$ cm^{-1} at the HF/6-31+G* level and $\sim 8 \pm 6$ cm^{-1} at the B3LYP/6-31+G* level. A very good accordance is also obtained between the calculated and experimental shifts upon adsorption. The mean deviations are $\sim 6 \pm 3$ cm^{-1} and $\sim 5 \pm 3$ cm^{-1} with HF and B3LYP methods, respectively. These results show the larger accurateness of the B3LYP method with respect to the HF one. This general good accordance between calculations and experiment concerning not only the absolute frequencies, but also the frequency shifts on going from free to adsorbed

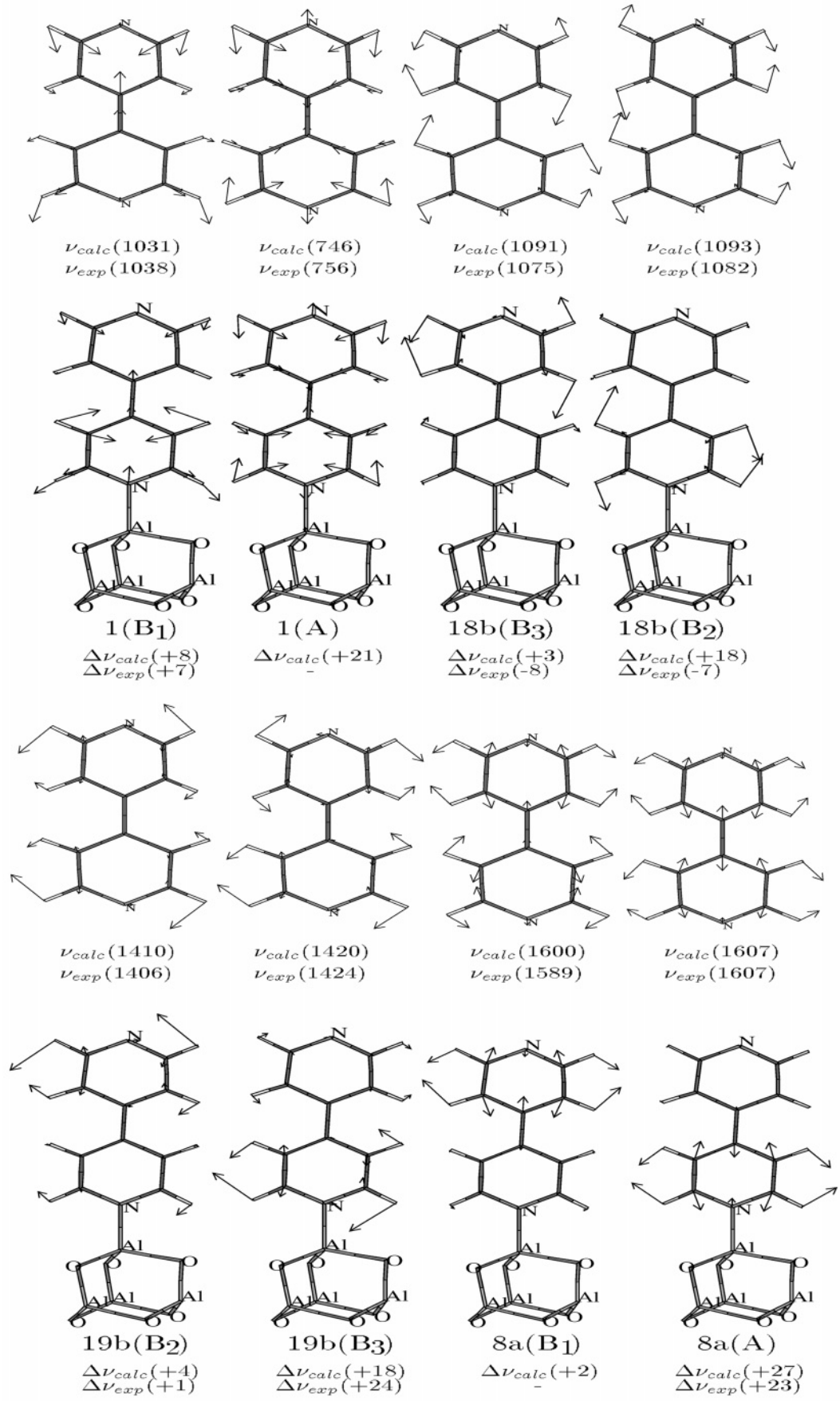

Figure 4. Calculated vibrational patterns of some in-plane normal modes of free and adsorbed 44BPY on Al_4O_6 cluster in the 700−1650 cm^{-1} spectral region. Numbers indicate the observed and calculated frequencies and frequency shifts in cm^{-1}. The scale for the arrows (displacements) is arbitrary but common to all the normal modes.

44BPY, shows that the changes in the force fields and the redistributions of potential energy upon adsorption are accurately computed. This validates the optimized geometry obtained for 44BPY adsorbed on alumina with HF and B3LYP methods.

As indicated by Table 8, and as yet previously shown, in free 44BPY, the potential energy is equally distributed on each pyridyl ring. On the other hand, upon adsorption, the two pyridyl rings lose their electronic equivalency. For all modes (except for mode 1 of b_1 symmetry in free 44BPY), the same coordinates contribute to the PEDs of free and adsorbed 44BPY, but with different distributions among both rings.

For mode 3, the energy is only slightly differently shared among both pyridyl rings. For modes 9a, 19a, and 8b, the loss of electronic equivalency between the rings is much more largely pronounced. Frequencies of all these modes (3, 9a, 19a, and 8b) are only slightly modified upon adsorption. This may be accounted for by the weak variations upon adsorption of the force constants relative to the coordinates (Table 2S) involved in the PEDs of these modes (Table 8) As for adsorbed PY, downward shifts might be expected for components of modes 19a and 8b, of which potential energy is predominantly shared among the pyridyl ring bound to alumina. Indeed, these modes involve the N_1C_2 coordinate of the bound ring. However, though the N_1C_2 length of the bound ring largely increases upon adsorption (Table 3), the relative force constant slightly decreases with Al_4O_6 or even increases with $Al(OH)_3$ (Table 2S).

For each component of modes 18b, 19b, and 8a, the energy is exclusively distributed among one pyridyl ring. The frequencies of the components of which potential energy is shared among the unbound pyridyl ring are only slightly shifted. Indeed, the force constants related to all of the coordinates of the unbound ring vary very weakly (Table 2S). Conversely, the frequencies of the components of the modes of which energy is distributed among the bound pyridyl ring are significantly upward shifted, according to calculations. For modes 19b and 8a (of b_3 and a symmetry in free 44BPY, respectively), the experimental positive shifts are very well reproduced by calculations, particularly by those considering the Al_4O_6 cluster at the B3LYP level ($\Delta\nu_{exp} = 24$ cm^{-1}, $\Delta\nu_{calc} = 18$ cm^{-1} for mode 19b; $\Delta\nu_{exp} = 23$ cm^{-1}, $\Delta\nu_{calc} = 27$ cm^{-1} for mode 8a). As in the case of PY, these shifts result from the significant increase of the force constant related to the R_2 coordinate, especially on going from free 44BPY to 44BPY adsorbed on Al_4O_6 cluster (Table 2S).

For mode 18b (of b_2 symmetry in free 44BPY), as for modes 19b and 8a, the R_2 contribution explains the upward shift calculated for this mode. This computed positive shift is in disagreement with experiment ($\Delta\nu_{exp} = -7$ cm^{-1}, $\Delta\nu_{calc} \sim 18$ cm^{-1} at B3LYP level and $\sim$24 cm^{-1} at HF level). However, it is to be noted that the experimental frequency related to mode 18b of adsorbed 44BPY is assigned to a shoulder, of which position is not clearly distinguishable.[26]

Finally, for the two components of mode 1 of adsorbed 44BPY, the potential energy is principally distributed among the bound pyridyl ring. Frequency of mode 1 (of b_1 symmetry in free 44BPY) is only slightly shifted, in accordance with experiment, due to the small variation of the force constant related to the S_1 coordinate. The calculated frequency of mode 1 of adsorbed 44BPY (of a symmetry in free 44BPY) is significantly upward shifted, particularly with Al_4O_6 cluster ($\Delta\nu_{calc} = 21$ cm^{-1}). It is not clearly interpreted by the analysis of the PEDs, as the force constants relative to the implied coordinates are only slightly modified upon adsorption. Unfortunately, the experimental frequency is unknown.

VI. Conclusions

Several conclusions may be drawn from this work. First, our results have shown that the calculated adsorption energies of PY and 44BPY complexed to the Al Lewis site of alumina clusters are nearly identical. This indicates that this characteristic depends only on the pyridyl ring (of the 44BPY molecule) that binds to the surface. The corrected adsorption energies are only slightly sensitive to the basis set and electron correlation effects, whereas they depend on the size and shape of the cluster model. However, the ESP analysis reveals that the charge-transfer effects are more important in PY and 44BPY Lewis complexes formed with the Al_4O_6 cluster than formed with hydrogenated clusters $Al(OH)_3$, $Al_4O_9H_6$, and $Al_{10}O_{21}H_{12}$ Consequently, the adsorption energies of PY and 44BPY complexes to Al_4O_6 cluster ($\sim$46 kcal/mol), which compare very well to experiment,[92] are strongly larger than those complexed to $Al(OH)_3$ ($\sim$32 kcal/mol), $Al_4O_9H_6$, and $Al_{10}O_{21}H_{12}$ ($\sim$25 kcal/mol) clusters. The non-hydrogenated cluster Al_4O_6 is more adapted to represent the ionic charater of alumina surface than the hydrogenated clusters. Thus, we conclude that the adsorption energies depend more on the ionic character of the cluster model than on its size.

Second, no pronounced dependence of the frequency shifts on the diffuse functions and on the electron correlation is found. In the same way, the frequency shifts are not sensitive to the size and to the shape of the clusters. This suggests that the interactions responsible for these vibrational characteristics are very local and that the influence of the rest of the alumina surface may be neglected.

Finally, the good agreement found between our calculated frequency shifts and the FT-IR data validates the cluster model approximation in studying specially the vibrational properties of these adsorbed molecules on alumina surfaces.

Supporting Information Available: Diagonal force constants in free PY and PY adsorbed on different alumina clusters (Table S1) and diagonal force constants in free 44BPY and 44BPY adsorbed on different alumina clusters (Table S2). This material is available free of charge via the Internet at http://pubs.acs.org.

References and Notes

(1) Knözinger, H.; Ratnasamy, P. *Catal. Rev. Sci. Eng.* **1978**, *17*, 31.
(2) Gautier, M.; Renaud, G.; Pham Van, L.; Villette, B.; Pollak, M.; Thromat, N.; Jollet, F.; Duraud, J. P. *J. Am. Ceram. Soc.* **1994**, *77*, 323.
(3) Paukshtis, E. A.; Yurchenko, E. N. *Russ. Chem. Rev.* **1983**, *52*, 242.
(4) Morterra, C.; Magnacca, G. *Catal. Today* **1996**, *27*, 497.
(5) Lercher, J. A.; Gründling, C.; Eder-Mirth, G. *Catal. Today* **1996**, *27*, 353.
(6) Busca, G. *Catal. Today* **1998**, *41*, 191.
(7) (a) Nelson, C. E.; Elam, J. W.; Cameron, M. A.; Tolbert, M. A.; George, S. M. *Surf. Sci.* **1998**, *416*, 341. (b) Liu, P.; Kendelewicz, T.; Brown, G. E., Jr.; Nelson, E. J.; Chambers, S. A. *Surf. Sci.* **1998**, *417*, 53.
(8) Hass, K. C.; Schneider, W. F.; Curioni, A.; Andreoni, W. *Science* **1998**, *282*, 265.
(9) Pelmenschikov, A. G.; van Santen, R. A.; Jänchen, J.; Meijer, E. *J. Phys. Chem.* **1993**, *97*, 11071.
(10) Shen, Y. F.; Suib, S. L.; Deeba, M.; Koermer, G. S. *J. Catal.* **1994**, *146*, 483.
(11) Lahousse, C.; Aboulayt, A.; Maugé, F.; Bachelier, J.; Lavalley, J. C. *J. Mol. Catal.* **1993**, *84*, 283.
(12) (a) Morterra, C.; Chiorino, A.; Ghiotti, G.; Garrone, E. *J. Chem. Soc., Faraday Trans. 1*, **1979**, *75*, 271. (b) Morterra, C.; Coluccia, S.; Chiorino, A.; Boccuzzi, F. *J. Catal.* **1978**, *54*, 348.

(13) Nortier, P.; Fourre, P.; Mohammed Saad, A. B.; Saur, O.; Lavalley, J. C. *Appl. Catal.* **1990**, *61*, 141.
(14) Haneda, M.; Joubert, E.; Ménézo, J. C.; Duprez, D.; Barbier, J.; Bion, N.; Daturi, M.; Saussey, J.; Lavalley, J. C.; Hamada, H. *Phys. Chem. Chem. Phys.* **2001**, *3*, 1366.
(15) Parry, E. P. *J. Catal* **1963**, *2*, 371.
(16) Satsuma, A.; Kamiya, Y.; Westi, Y.; Hattori, T. *Appl. Catal. A: General* **2000**, *194*−*195*, 253.
(17) Wachs, I. E. *Colloids Surf. A: Physicochem. Eng. Aspects* **1995**, *105*, 143.
(18) Hendra, P. J.; Turner, I. D. M.; Loader, E. J.; Stacey, M. *J. Phys. Chem.* **1974**, *78*, 300.
(19) (a) Zaki, M. I.; Hasan, M. A.; Al-Sagheer, F. A.; Pasupulety, L. *Colloids Surf. A: Physicochem. Eng. Aspects* **2001**, *190*, 261. (b) Zaki, M. I.; Hasan, M. A.; Al-Sagheer, F. A.; Pasupulety, L. *Langmuir* **2000**, *16*, 430. (c) Zaki, M. I.; Hasan, M. A.; Pasupulety, L. *Langmuir* **2001**, *17*, 768.
(20) Wragg, J. L.; White, H. W.; Sutcu, L. F. *Phys. Rev. B* **1988**, *37*, 2508.
(21) Sarbak, Z. *Appl. Catal. A: General* **1997**, *159*, 147.
(22) Sachett, C. M. M.; Da Silva, P. N.; Lam, Y. L.; Dufaux, M.; Frety, R.; Primet, M. *Bull. Soc. Chim. Fr.* **1989**, *3*, 357.
(23) Pichat, P.; Mathieu, M. V.; Imelik, B. *Bull. Soc. Chim. Fr.* **1969**, *8*, 2611.
(24) Bagshaw, S. A.; Cooney, R. P. *Appl. Spectrosc.* **1996**, *50*, 1319.
(25) Bagshaw, S. A.; Cooney, R. P. *J. Mater. Chem.* **1994**, *4*, 557.
(26) Bagshaw, S. A.; Cooney, R. P. *Appl. Spectrosc.* **1996**, *50*, 310.
(27) Gorb, L. G.; Gunko, V. M.; Goncharuk, V. V.; Karakhim, S. A. *React. Kinet. Catal. Lett.* **1989**, *38*, 21.
(28) Mardilovich, P. P.; Zelenkovskii, V. M.; Lysenko, G. N.; Trokhimetz, A. I.; Zhidomirov, G. M. *React. Kinet. Catal. Lett.* **1988**, *36*, 107.
(29) Fleisher, M. B.; Golender, L. O.; Shimanskaya, M. V. *J. Chem. Soc., Faraday Trans.* **1991**, *87*, 745.
(30) Wittbrodt, J. M.; Hase, W. L.; Schlegel, H. B. *J. Phys. Chem. B* **1998**, *102*, 6539.
(31) Shapovalov, V.; Truong, T. N. *J. Phys. Chem. B* **2000**, *104*, 9859.
(32) Nygren, M. A.; Gay, D. H.; Richard, C.; Catlow, A. *Surf. Sci.* **1997**, *380*, 113.
(33) Fernandez Sanz, J.; Rabaa, H.; Poveda, F. M.; Marquez, A. M.; Calzado, C. J. *Int. J. Quantum Chem.* **1998**, *70*, 359.
(34) Tachikawa, H.; Tsuchida, T. *J. Mol. Catal. A: Chemical* **1995**, *96*, 277.
(35) (a) Lindblad, M.; Pakkanen, T. A. *Surf. Sci.* **1993**, *286*, 333. (b) Hirva, P.; Pakkanen, T. A. *Surf. Sci.* **1992**, *271*, 530.
(36) Casarin, M.; Maccato, C.; Vittadini, A. *Inorg. Chem.* **2000**, *39*, 5232.
(37) Neyman, K. M.; Nasluzov, V. A.; Zhidomirov, G. M. *Catal. Lett.* **1996**, *40*, 183.
(38) Nasluzov, V. A.; Rivanenkov, V. V.; Shor, A. M.; Neyman, K. M.; Birkenheuer, U.; Rösch, N. *Int. J. Quantum Chem.* **2002**, *90*, 386.
(39) Bates, S.; Dwyer, J. *J. Phys. Chem.* **1993**, *97*, 5897.
(40) Maresca, O.; Allouche, A.; Aycard, J. P.; Rajzman, M.; Clemendot, S.; Hutschka, F. *J. Mol. Struct. (THEOCHEM)* **2000**, *505*, 81.
(41) Rodriguez, J. A.; Chaturvedi, S.; Kuhn, M.; Hrbek, J. *J. Phys. Chem. B* **1998**, *102*, 5511.
(42) Hirva, P.; Pakkanen, T. A. *Surf. Sci.* **1992**, *277*, 389.
(43) (a) Kawakami, H.; Yoshida, S. *J. Chem. Soc., Faraday Trans. 2* **1985**, *81*, 1117. (b) Kawakami, H.; Yoshida, S. *J. Chem. Soc., Faraday Trans. 2* **1985**, *81*, 1129. (c) Kawakami, H.; Yoshida, S. *J. Chem. Soc., Faraday Trans. 2* **1986**, *82*, 1385.
(44) Nortier, P.; Borosy, A. P.; Allavena, M. *J. Phys. Chem. B* **1997**, *101*, 1347.
(45) (a) Borosy, A. P.; Silvi, B.; Allavena, M.; Nortier, P. *J. Phys. Chem.* **1994**, *98*, 13189. (b) Wander, A.; Searle, B.; Harrison, N. M. *Surf. Sci.* **2000**, *458*, 25. (c) Baxter, R.; Reinhardt, P.; Lopez, N.; Illas, F. *Surf. Sci.* **2000**, *445*, 448. (d) Gomes, J. R. B.; Moreira, I. de P. R.; Reinhardt, P.; Wander, A.; Searle, B. G.; Harrison, N. M.; Illas, F. *Chem. Phys. Lett.* **2001**, *341*, 412. (e) Carrasco, J.; Gomes, J. R. B.; Illas, F. *Phys. Rev. B* **2004**, *69*.
(46) (a) Kassab, E.; Jessri, H.; Allavena, M.; White, D. *J. Phys. Chem. A* **1999**, *103*, 2766. (b) Boronat, M.; Viruela, P.; Corma, A. *J. Phys. Chem. A* **1998**, *102*, 982. (c) Brändle, M.; Sauer, J. *J. Am. Chem. Soc.* **1998**, *120*, 1556.
(47) Frisch, M. J.; Trucks, G. W.; Schlegel, H. B.; Scuseria, G. E.; Robb, M. A.; Cheeseman, J. R.; Zakrzewski, V. G.; Montgomery, J. A., Jr.; Stratmann, R. E.; Burant, J. C.; Dapprich, S.; Millam, J. M.; Daniels, A. D.; Kudin, K. N.; Strain, M. C.; Farkas, O.; Tomasi, J.; Barone, V.; Cossi, M.; Cammi, R.; Mennucci, B.; Pomelli, C.; Adamo, C.; Clifford, S.; Ochterski, J.; Petersson, G. A.; Ayala, P. Y.; Cui, Q.; Morokuma, K.; Malick, D. K.; Rabuck, A. D.; Raghavachari, K.; Foresman, J. B.; Cioslowski, J.; Ortiz, J. V.; Baboul, A. G.; Stefanov, B. B.; Liu, G.; Liashenko, A.; Piskorz, P.; Komaromi, I.; Gomperts, R.; Martin, R. L.; Fox, D. J.; Keith, T.; Al-Laham, M. A.; Peng, C. Y.; Nanayakkara, A.; Gonzalez, C.; Challacombe, M.; Gill, P. M. W.; Johnson, B. G.; Chen, W.; Wong, M. W.; Andres, J. L.; Gonzalez, C.; Head-Gordon, M.; Replogle, E. S.; Pople, J. A. *Gaussian 98*, revision A.5; Gaussian, Inc.: Pittsburgh, PA, 1998.
(48) Breneman, C. M.; Wiberg, K. B. *J. Comput. Chem.* **1990**, *11*, 361.
(49) Boys, S. F.; Bernardi, F. *Mol. Phys.* **1970**, *19*, 553.
(50) (a) Allouche, A. REDONG (*QCPE628*) **1992**. (b) Allouche, A.; Pourcin, J. *Spectrochim. Acta A* **1993**, *49*, 571.
(51) Pulay, P.; Fogarasi, G.; Pang F.; Boggs, J. E. *J. Am. Chem. Soc.* **1979**, *101*, 2550.
(52) Poizat, O.; Ventura, M.; Buntinx, G. *Spectrosc. Lett.* **1990**, *23*, 701.
(53) Poizat, O.; Buntinx, G.; Ventura, M.; Lautié, M. F. *J. Phys. Chem.* **1991**, *95*, 1245.
(54) Poizat, O.; Buntinx, G.; Valat, P.; Wintgens, V.; Bridoux, M. *J. Phys. Chem.* **1993**, *97*, 5905.
(55) Ould-Moussa, L.; Poizat, O.; Castellà-Ventura, M.; Buntinx, G.; Kassab, E. *J. Phys. Chem.* **1996**, *100*, 2072.
(56) Castellà-Ventura, M.; Kassab, E. *J. Raman Spectrosc.* **1998**, *29*, 511.
(57) Almenningen, A.; Bastiansen, O. *K. Nor. Vidensk. Selsk. Skr.* **1958**, *4*, 1.
(58) Mata, F.; Quintana, M. J.; Sorensen, G. O. *J. Mol. Struct.* **1977**, *42*, 1.
(59) Pyckhout, W.; Horemans, N.; Van Alsenoy, C.; Geise, H. J.; Rankin, D. W. H. *J. Mol. Struct.* **1987**, *156*, 315.
(60) Wiberg, K. B.; Walters, V. A.; Wong, K. N.; Colson, S. D. *J. Phys. Chem.* **1984**, *88*, 6067.
(61) Kjaergaard, H. G.; Proos, R. J.; Turnbull, D. M.; Henry, B. R. *J. Phys. Chem.* **1996**, *100*, 19273.
(62) Szczepaniak, K.; Chabrier, P.; Person, W. B.; Del Bene, J. E. *J. Mol. Struct.* **1997**, *436*−*437*, 367.
(63) Szafran, M.; Koput, J. *J. Mol. Struct.* **2001**, *565*−*566*, 439.
(64) Experimental values of the Al−O distances are 1.72 Å in the tetrahedron and 1.95 Å in the octahedron: Wyckoff, R. W. G. *Crystal Structures*, 2nd ed.; Interscience: New York, 1968; Vol. 4.
(65) Scott, A. P.; Radom, L. *J. Phys. Chem.* **1996**, *100*, 16502.
(66) Castellà-Ventura, M.; Kassab, E.; Buntinx, G.; Poizat, O. *Phys. Chem. Chem. Phys.* **2000**, *2*, 4682.
(67) Ould-Moussa, L.; Castellà-Ventura, M.; Kassab, E.; Poizat, O.; Strommen, D. P.; Kincaid, J. R. *J. Raman Spectrosc.* **2000**, *31*, 377.
(68) Guo, H.; Karplus, M. *J. Chem. Phys.* **1988**, *89*, 4235.
(69) Corrsin, L.; Fax, B. J.; Lord, R. C. *J. Chem. Phys.* **1953**, *21*, 1170.
(70) Wilmshurst, J. K.; Bernstein, H. J. *Can. J. Chem.* **1957**, *35*, 1183.
(71) McCullough, J. P.; Douslin, D. R.; Messerly, J. F.; Hossenlopp, I. A.; Kincheloe, T. C.; Waddington, G. *J. Am. Chem. Soc.* **1957**, *79*, 4289.
(72) Loisel, J.; Lorenzelli, V. *J. Mol. Struct.* **1967**, *1*, 157.
(73) DiLella, D. P.; Stidham, H. D. *J. Raman Spectrosc.* **1980**, *9*, 90.
(74) Wong, K. N.; Colson, S. D. *J. Mol. Spectrosc* **1984**, *104*, 129.
(75) Klots, T. D. *Spectrochim. Acta A* **1998**, *54*, 1481.
(76) Long, D. A.; Murfin, F. S.; Hales, J. L.; Kynaston, W. *J. Chem. Soc., Faraday Trans.* **1957**, *53*, 1171.
(77) Popov, A. I.; Marshall, J. C.; Stute, F. B.; Person, W. B. *J. Am. Chem. Soc.* **1961**, *83*, 3586.
(78) Pongor, G.; Pulay, P.; Fogarasi, G.; Boggs, J. E. *J. Am. Chem. Soc.* **1984**, *106*, 2765.
(79) Pongor, G.; Fogarasi, G.; Boggs, J. E.; Pulay, P. *J. Mol. Spectrosc.* **1985**, *114*, 445.
(80) Dkhissi, A.; Adamowicz, L.; Maes, G. *J. Phys. Chem. A* **2000**, *104*, 2112.
(81) Barone, V. *J. Phys. Chem. A* **2004**, *108*, 4146.
(82) Abbattista, F.; Delmastro, S.; Gozzelino, G.; Mazza, D.; Vallino, M.; Busca, G.; Lorenzelli, V.; Ramis, G. *J. Catal.* **1989**, *117*, 42.
(83) Di Felice, R.; Northrup, J. E. *Phys. Rev. B* **1999**, *60*, R16 287.
(84) Varsanyi, G. In *Assignments for Vibrational Spectra of Seven Hundred Benzene Derivatives*; Lang, L, Ed.; Adam Hilger: London, 1974; Vol. 1.
(85) Wilson, E. B. *Phys. Rev.* **1934**, *45*, 706.
(86) Emsley, J. W.; Stephenson, D. S.; Lindon, J. C.; Lunazzi, L.; Pulga, S. *J. Chem. Soc., Perkin Trans. 2* **1975**, *14*, 1541.
(87) (a) Barone, V.; Lelj, F.; Cauletti, C.; Piancastelli, M. N.; Russo, N. *Mol. Phys.* **1983**, *49*, 599. (b) Barone, V.; Lelj, F.; Commisso, L.; Russo, N.; Cauletti, C.; Piancastelli, M. N. *Chem. Phys.* **1985**, *96*, 435.
(88) Ribeiro Da Silva, M. A. V.; Morais, V. M. F.; Matos, M. A. R.; Rio, C. M. A. *J. Org. Chem.* **1995**, *60*, 5291.
(89) (a) Foglizzo, R.; Novak, A. *J. Chim. Phys.* **1969**, *66*, 1539. (b) Glazunov, V. P.; Odinokov, S. E. *Spectrochim. Acta A* **1982**, *38*, 399.
(90) Spinner, E. *Aust. J. Chem.* **1967**, *20*, 1805.
(91) Ferwerda, R.; Maas, J. H. v. d.; Duijneveldt, F. B. v. *J. Mol. Catal. A: Chem.* **1996**, *104*, 319.
(92) Clark, A.; Holm, V. C. F.; Blackburn, D. M. *J. Catal.* **1962**, *1*, 244.
(93) (a) Kevorkian, V.; Steiner, R. O. *J. Phys. Chem.* **1963**, *67*, 545. (b) Stone, F. S.; Whalley, L. *J. Catal.* **1967**, *8*, 173.